ISSN 0021-3640, JETP Letters, 2015, Vol. 102, No. 4, pp. 203–206. © Pleiades Publishing, Inc., 2015.

FIELDS, PARTICLES, AND NUCLEI

Anisotropy of the Fission Fragments from Neutron-Induced Fission in the Intermediate Energy Range of 1–200 MeV[1]

A. S. Vorobyev[a, *], A. M. Gagarski[a], O. A. Shcherbakov[a], L. A. Vaishnene[a], and A. L. Barabanov[b, c]

[a] *Petersburg Nuclear Physics Institute, National Research Centre Kurchatov Institute, Gatchina, 188300 Russia*

[b] *National Research Centre Kurchatov Institute, Moscow, 123182 Russia*

[c] *Moscow Institute of Physics and Technology (State University), Dolgoprudnyi, Moscow region, 141700 Russia*

**e-mail: alexander.vorobyev@pnpi.spb.ru*

Received June 15, 2015; in final form, July 10, 2015

Angular distributions of fission fragments from the neutron-induced fission of ^{232}Th, ^{235}U, and ^{238}U have been measured in the energy range 1–200 MeV at the neutron time-of-flight (TOF) spectrometer GNEIS using position sensitive multiwire proportional counters as fission fragment detector. A short description of the experimental equipment and measurement procedure is given. The anisotropy of fission fragments deduced from the data on measured angular distributions is presented in comparison with experimental data of other authors.

DOI: 10.1134/S0021364015160134

Angular distributions of fission fragments and cross sections of nuclear neutron-induced fission are the main source of information about fission barrier structure and nuclear transitional states on the barrier. The relevant experimental data have been accumulated over decades, mostly for $E_n < 20$ MeV (E_n is the energy of incident neutrons). These data are not only of high scientific value, but of great significance for nuclear technologies as well. However, nowadays discussion on accelerator-driven systems (for nuclear power generation and nuclear transmutation) has created considerable interest to nuclear fission at intermediate ($E_n < 200$ MeV) and higher neutron energies.

In this paper new experimental data on angular distributions of fragments from fission of target nuclei ^{232}Th, ^{235}U, and ^{238}U by neutrons with energies 1–200 MeV are presented. Measurements were carried out at 36 m flight path of a neutron time-of-flight (TOF) spectrometer GNEIS [1] utilizing the PNPI 1 GeV proton synchrocyclotron as a pulsed high-intensity spallation neutron source. Previously, the neutron-induced fission cross sections have been measured at the GNEIS facility for ^{233}U, ^{235}U, ^{238}U, ^{232}Th, ^{239}Pu, ^{240}Pu, ^{237}Np, ^{243}Am, ^{209}Bi, Pb, and W nuclei in the same energy range 1–200 MeV [2, 3] using the parallel plate fission ionization chamber (FIC) as a fission fragment detector. Analysis of the experimental data obtained with the FIC has shown the necessity of considering a correction for fragment anisotropy in the calculation of the FIC registration efficiency (the corrections on fragment anisotropy were used in the determination of the ^{238}U/^{235}U fission cross section ratio for $E_n < 1$ GeV at the n_TOF facility at CERN [4]).

Schematic view of experimental setup is shown in Fig. 1. In the present measurements we used fissile targets 120 × 120 mm^2 of size made by vacuum deposition of Th and U tetrafluorides on 2 μm Mylar foil. Their thicknesses were 100–150 μg/cm^2. Two coordinates sensitive multiwire proportional counters (MWPC) 140 × 140 mm^2 of size [5] were used for fission fragment registration. The detectors were placed close to the target in the beam one after the other. The neutron beam diameter at the target position was equal to 75 mm. The neutron beam axis came through the geometrical centers of the target and MWPC's electrodes being perpendicular to them. A value of cos(θ), where θ is an angle between neutron beam axis and fission fragment momentum, can be derived easily from the coordinates of the fission fragment measured with two detectors. Each one of the MWPCs consists of X and Y anodes wire planes made of 25 microns gilded tungsten wires and common cathode located between them. The cathode is made as a square mesh from the same wires. The wire spacing is 1 mm and anode-cathode gaps are about 3 mm. Every two (of 140) neighboring anode wires are connected to the 70 taps of delay line with a specific delay of 2 ns/step for coordinate information readout. The timing signals from corresponding ends of the delays carry position information. The coordinates are proportional to the time differences between cathode and

[1] The article is published in the original.

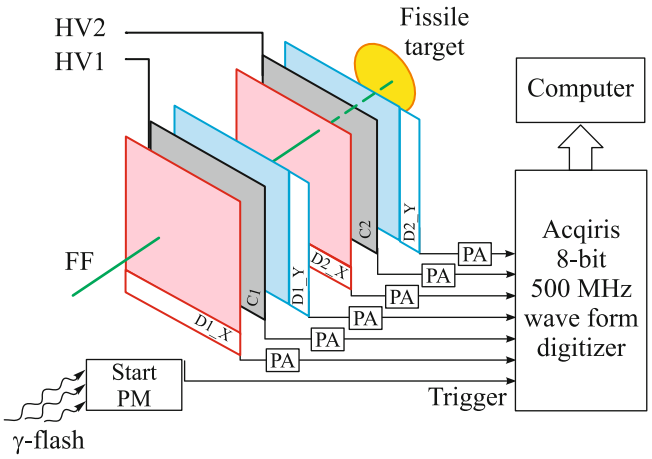

Fig. 1. (Color online) Schematic view of the experimental setup: (PA) preamplifier; (PM) photomultiplier; (HV) high voltage; (FF) fission fragment; (D1_X, D2_X) detectors 1, 2 (*X* axis); (D1_Y, D2_Y) detectors 1, 2 (*Y* axis); (C1, C2) cathode 1, 2.

anode signals. The two MWPC cathodes were installed at distance of 9 mm from each other, and the cathode of the first MWPC was 6 mm apart from the target. The detectors arrangement used in the present measurements enables to cover the interval $0.3 < \cos(\theta) < 1.0$. As it follows from Monte-Carlo simulation, in this range the setup efficiency is almost constant. The data with $\cos(\theta) < 0.3$ are much less accurate due to a sharp decrease in the registration efficiency. The cathode signals were used as STOP signals for the neutron TOF-spectroscopy, whereas a "bare" photomultiplier FEU-30, being installed at the neutron beam 1 m downstream the MWPC, produced START signal due to registration of a "gamma-flash."

A readout system (Fig. 1) used three outputs from each MPWC, which were fed through the fast preamplifiers into 2 waveform digitizers (Acqiris DC-270, 8-bit resolution, 500 Ms/s sampling rate). The digitizers were triggered by signals from START photomultiplier for each accelerator pulse. The waveforms were stored on computer hard disk for offline reduction. Time and pulse-height analyses of the waveforms allowed to derive the neutron energy and the fission fragment coordinates on the MWPCs, and, hence, the angle information.

The anisotropy parameters $W(0°)/W(90°)$ of angular distributions of fission fragments in the center-of-mass system were deduced from the data on measured angular distributions in the laboratory system ($\cos(\theta)$ bins were equal to 0.01) by fitting them in the range $0.4 < \cos(\theta) < 1.0$ with the expression $W(\theta) \sim 1 + b\cos^2(\theta)$, where $b = W(0°)/W(90°) - 1$. It should be noted that the geometrical acceptance of the experimental setup is the $\cos(\theta) > 0.3$ range but the fitting range is the $\cos(\theta) > 0.4$ range where the setup efficiency registration is constant and, therefore, the result is not dependent on the efficiency uncertainty, and is not necessary to take into account any additional corrections to the measured angular distribution. To take into account the linear momentum contribution into the measured angular distribution, the anisotropy parameters obtained from the data accumulated with two setup orientations relative to the beam direction (downstream and upstream) have been averaged. Figure 2 shows angular distributions for ^{232}Th, averaged over two setup orientation relative to the neutron beam, obtained in neutron energy intervals 6.8 ± 0.2 and 128 ± 12 MeV and the results of their fit. The anisotropy parameters are shown in Figs. 3–5 in comparison with the experimental data of other authors. The error bars shown include both statistical and systematic errors. The statistical errors were

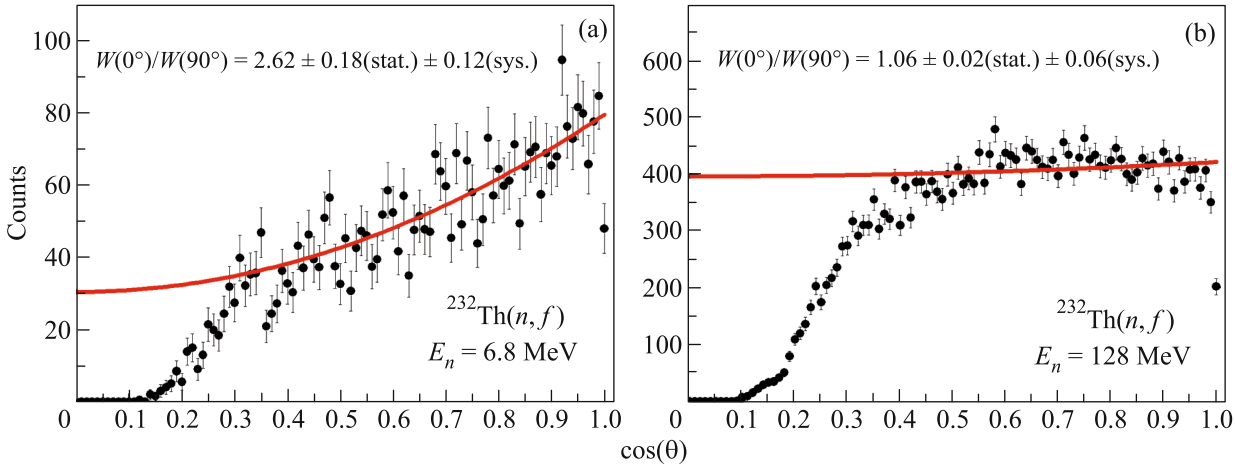

Fig. 2. (Color online) Example of angular distributions for ^{232}Th. The error bars represent statistical uncertainties. The solid line is a result of the fitting by the function $W(\theta) \sim 1 + b\cos^2(\theta)$.

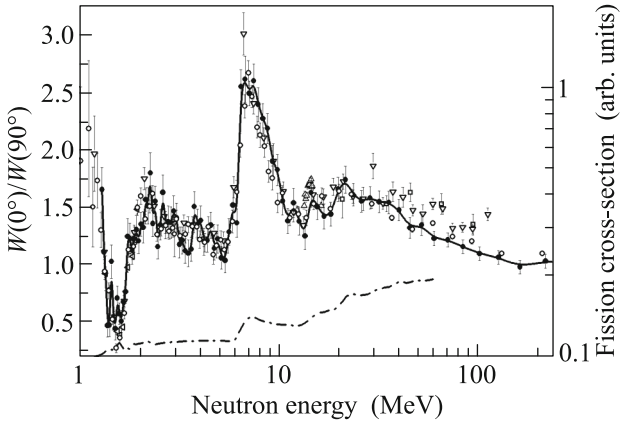

Fig. 3. Anisotropy of fission fragments of ^{232}Th according to (▽) [6], (◁) [19], (△) [11], (□) [7], (○) [8], (●) present data, and (–●–) fission cross section [9].

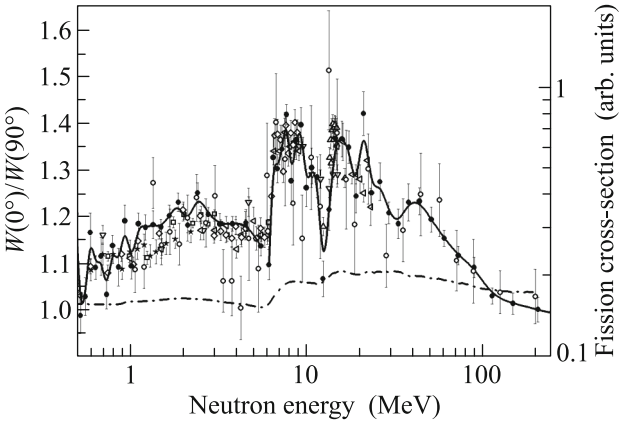

Fig. 4. Anisotropy of fission fragments of ^{235}U according to (▽) [12], (◁) [14], (△) [11], (◇) [15], (★) [10], (□) [13], (○) [8], (●) present data, and (–●–) fission cross section [9].

obtained directly from the fitting procedure. The systematical errors were estimated as a difference between anisotropy parameters obtained using two angular ranges for fitting: $0.4 < \cos(\theta) < 1.0$ and $0.48 < \cos(\theta) < 1.0$. A solid line connecting present data points is used solely for convenience of presentation.

It must be admitted that near the fission threshold as well as for lower energies, a contribution of the fourth Legendre polynomial (or, more simply, of the term $\sim\cos^4(\theta)$) into the fragment angular distribution can be sizable (see, for example, Fig. 3 in [6]). However, at higher energies only the 2nd polynomial is of significance (see Fig. 2). Since this work is mainly dedicated to the high energies, we used only the term $\sim\cos^2(\theta)$ for fitting the data. Thus, in principle, there exists some additional uncertainty for anisotropy parameter in the narrow energy range near the fission threshold and below. Nevertheless, even in this range, $E_n = (1–2)$ MeV, as it follows from Fig. 3, there is an agreement (within the experimental uncertainties) of our data for ^{232}Th and the data by Tarrio et al. [6] obtained with an account for the 4th Legendre polynomial.

Turning to the discussion of the obtained results, we note that until recently in the energy range 20–100 MeV only the data by Ryzhov et al. [7] on the angular anisotropy of fission fragments for ^{232}Th and ^{238}U isotopes existed, while there were no data for neutron-induced fission of ^{235}U. It is also of interest that a significant difference in fission fragment angular anisotropy was observed for ^{232}Th and ^{238}U isotopes with the use of quasi-monochromatic neutron source [7]. The TOF spectrometers seem more appropriate, but currently only two neutron TOF facilities, namely, the GNEIS at PNPI and n_TOF at CERN, which enable to cover a whole energy range 1–200 MeV in a single measurement, are used for the measurements of fission fragment anisotropy.

At CERN, the studies of angular anisotropy of fission fragments were performed for a number of nuclei in the energy range up to 200 MeV, however, the situation with the data is ambiguous. For ^{232}Th isotope, the results by Leong [8] and Tarrio et al. [6] have small experimental errors, but differ significantly from each other (these data are shown in Fig. 3). At the same time, for the nuclei of ^{235}U and ^{238}U there are only the data by Leong, but they have high experimental errors (these data are shown in Figs. 4 and 5). Notice that in [4] by Paradela et al. (n_TOF collaboration), only the old data [7] were used for the fission fragment angular anisotropy (i.e., only for ^{238}U isotope in the energy range up to 100 MeV).

Our results may be summarized as follows:

(i) for all three nuclei the energy-dependent structure of the anisotropy demonstrates a strong correla-

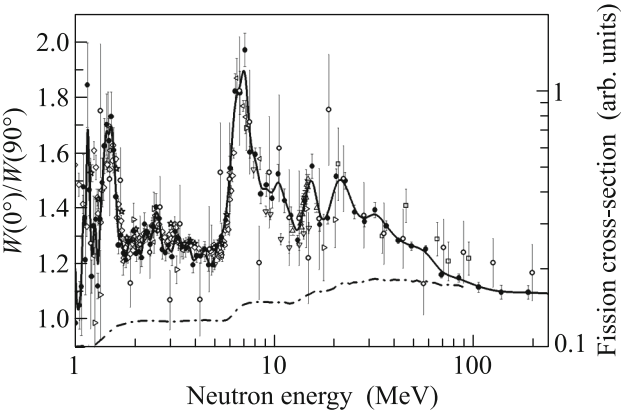

Fig. 5. Anisotropy of fission fragments of ^{238}U according to (▽) [12], (◁) [14], (▷) [16], (△) [11], (◇) [17], (★) [18], (□) [7], (○) [8], (●) present data, and (–●–) fission cross section [9].

tion with the well-known step-like structure of fission cross section [9] (shown in Figs. 3–5 by dash-dot line). Namely, the anisotropy coefficient increases with the opening of each fission chance (n, f), (n, nf), $(n, 2nf)$, etc.;

(ii) in the low energy range up to 20 MeV, our data agree well with the numerous previously obtained results [10–19]. This confirms the reliability of the used method of measurement of angular distributions of fission fragments;

(iii) in the energy range 20–100 MeV, we do not endorse the result shown by Ryzhov et al. [7] about a significant difference in the $W(0°)/W(90°)$ for ^{232}Th and ^{238}U. On the contrary, according to our data, the fission fragment anisotropies are approximately the same within the errors for these isotopes;

(iv) in the energy region 20–200 MeV, our data for ^{232}Th differ substantially from the n_TOF data given by Tarrio et al. [6], but show an agreement within the experimental errors with the n_TOF data given by Leong [8]. Uncertainties of our data for the ^{235}U and ^{238}U isotopes are much smaller than those presented by Leong.

We note in conclusion that our data points for ^{232}Th and ^{238}U isotopes in the intermediate energy range that are presented in Figs. 3 and 5, lie not only below the data by Ryzhov et al. [7], but below the theoretical curve obtained in the same paper in the framework of the standard statistical model with account for pre-equilibrium processes. This means that some elements of this model require revision. We plan to perform such an analysis and to describe the results obtained for ^{232}Th and ^{238}U isotopes with zero spins, as well as for ^{235}U nucleus with a relatively high initial spin $I = 7/2$.

We are grateful to E.M. Ivanov and the staff of the PNPI synchrocyclotron for their permanent assistance and friendly support. A valuable contribution of people from the Tracks Detectors Department and the Information Technologies and Automation Division of PNPI in manufacture of the MWPC is highly appreciated. The work of A.L.B. was supported in part by the Council of the President of the Russian Federation for Support of Young Scientists and Leading Scientific Schools (project no. NSh-932.2014.2).

REFERENCES

1. N. K. Abrosimov, G. Z. Borukhovich, A. B. Laptev, V. V. Marchenkov, G. A. Petrov, O. A. Shcherbakov, Yu. V. Tuboltsev, and V. I. Yurchenko, Nucl. Instrum. Methods Phys. Res. A **242**, 121 (1985).
2. O. A. Shcherbakov, A. Yu. Donets, A. V. Evdokimov, A. V. Fomichev, T. Fukahori, A. Hasegawa, A. B. Laptev, V. M. Maslov, G. A. Petrov, S. M. Soloviev, Yu. V. Tuboltsev, and A. S. Vorobyev, in *Proceedings of the International Conference on Nuclear Data for Science and Technology, October 7–12, 2001; Tsukuba, Ibaraki, Japan,* J. Nucl. Sci. Technol. **39**, 230 (2002).
3. A. B. Laptev, O. A. Shcherbakov, A. S. Vorobyev, R. C. Haight, and A. D. Carlson, in *Proceedings of the 4th International Conference on Fission and Properties of Neutron-Rich Nuclei, Sanibel Island, USA, November 11–17, 2007,* Ed. by J. H. Hamilton, A. V. Ramayya, and H. K. Carter (World Scientific, Singapore, 2008), p. 462.
4. C. Paradela, M. Calviani, D. Tarrio, E. Leal-Cidoncha, L. S. Leong, et al., Phys. Rev. C **91**, 024602 (2015).
5. G. F. Knoll, *Radiation Detection and Measurements,* 3rd ed. (Wiley, New York, 2000), p. 190.
6. D. Tarrio, L. S. Leong, L. Audouin, I. Duran, C. Paradela, et al., Nucl. Data Sheets **119**, 35 (2014).
7. I. V. Ryzhov, M. S. Onegin, G. A. Tutin, J. Blomgren, N. Olsson, A. V. Prokofiev, and P.-U. Renberg, Nucl. Phys. A **760**, 19 (2005).
8. L. S. Leong, PhD Thesis, CERN-Thesis-2013-254.
9. ENDF/B-VII.1, Nucl. Data Sheets **112**, 2887 (2011).
10. S. Ahmad, M. M. Islam, A. H. Khan, M. Kaliquzzaman, M. Husain, and M. A. Rahman, Nucl. Sci. Eng. **71**, 208 (1979).
11. Kh. D. Androsenko, G. G. Korolev, and D. L. Shpak, Vopr. At. Nauki Tekh., Ser. Yad. Konst. **46** (2), 9 (1982).
12. R. B. Leachman and L. Blumberg, Phys. Rev. **137**, B814 (1965).
13. V. G. Nesterov, G. N. Smirenkin, and D. L. Shpak, Sov. J. Nucl. Phys. **4**, 713 (1966).
14. J. E. Simmons and R. L. Henkel, Phys. Rev. **120**, 198 (1960).
15. J. W. Meadows and C. Budtz-Jorgensen, in *Proceedings of the Conference on Nuclear Data for Science and Technology, Antwerpen, 1982,* p. 740.
16. R. L. Henkel and J. E. Brolley, Jr., Phys. Rev. **103**, 1292 (1956).
17. D. L. Shpak, Sov. J. Nucl. Phys. **50**, 574 (1989).
18. F. Vives, F.-J. Hambsch, G. Barreau, S. Oberstedt, and H. Bax, Nucl. Phys. A **662**, 63 (2000).
19. J. Caruana, J. W. Boldeman, and R. L. Walsh, Nucl. Phys. A **285**, 205 (1977).